Estimating changes in radiation exposure and the risk zones size during an urban release event

Gustavo da Gama Souza[1,2], Claudio Antonio Federico[2], Jeferson da Silva Oliveira[2], Guilherme Gazolla Santana[1,2], Alan Bendasoli Pavan[3], Jonathan de Almeida Lapa[1,2], Felipe Lopes Frigi[1,2], Hektor Sthenos Alves Monteiro[3], Edson Ramos de Andrade[2,4,5,6]

[1]Instituto Tecnológico de Aeronáutica (ITA), São José dos Campos/SP – Brazil
[2]Instituto de Estudos Avançados (IEAv), São José dos Campos/SP – Brazil
[3]Universidade Federal de Itajubá (UNIFEI), Itajubá/MG – Brazil
[4]Universidade do Oeste Paulista (UNOESTE), Presidente Prudente/SP – Brazil
[5]Programa de Pós-Graduação em Engenharia de Defesa, Instituto Militar de Engenharia (IME), Rio de Janeiro/RJ – Brazil
[6]Programa de Pós-Graduação em Engenharia Nuclear, Instituto Militar de Engenharia (IME), Rio de Janeiro/RJ – Brazil

Abstract − **This study proposes a simple geometrical approach to identify areas of increased vulnerability and high-risk zones during the early stages of a radioactive urban event triggered by a radiological dispersal device (RDD). Rapid estimation of potentially affected areas, their location, and possible size and direction variations due to local atmospheric stability conditions, represented by the Pasquill-Gifford classification, is crucial. We conservatively estimate these zones and the radiological contamination using the trusted HotSpot Health Physics code version 3.1.2. The proposed methodology aims to estimate overlapping contamination areas due to changes in local atmospheric conditions. This provides valuable data for decision-making and strategy development, using computational simulations to reduce risks and minimize environmental impacts in the initial phase of such events. This research impacts urban planning, emergency response, and public safety measures, offering practical solutions to mitigate the effects of radiological dispersal events.**

Key-Words − **radiation release; computer simulation; local weather; risk zones**

I. Introduction

The initial hours of a radiological event are crucial in determining the best course of action to mitigate damage and minimize the impact on populations and critical infrastructures such as energy distribution networks, communications, and transportation. Determining zones of higher radiological vulnerability is crucial for modeling consequences when in situ measurements are unavailable. To shed light on this issue, we conducted a study that conservatively used computer modeling to simulate the release of radioactive material in an urban center and estimate the initial trends. The simulation employs an ellipse to represent the contamination zone for different levels of radiation exposure, known as isodoses. The shape and size of these contamination fields are determined by the local atmospheric conditions, which are classified using the Pasquill-Gifford (PG) model. The dimensions of these zones can be significantly affected by variations in the PG classes and wind direction, which can limit the accuracy of predictions and the ability of responders to cope with the radioactive contamination event. The analytical simulations were carried out using the HotSpot software (version 3.1.2) with Gaussian modeling [7]. This model provides a conservative approach to the event, contamination levels, and Total Effective Dose Equivalent (TEDE) that individuals in the public may be exposed to. The radioactive material released during the event is responsible for external, internal, or both types of exposure. HotSpot [7] was preferred over other available options due to its speed, user-friendly interface, availability, and the fact that it provides results that facilitate decision-making and initial coping strategies.

Therefore, this study considers the variations in PG classes and wind direction to identify the areas that remain at risk even under changing conditions. These overlapping areas are defined as the intersection between projected plumes from the exact origin resulting from variations in PG classes and wind direction in the impacted area. The main objective is to show how the number of people at risk can vary in contaminated areas depending on the wind direction and PG class. When the wind direction changes, the contaminated area's ellipse may not rotate enough to free the entire area, causing overlap with the previous state. This creates a transition zone where part of the land falls within both areas. The study aims to determine the impact of this zone on the potentially affected population as both the PG classes and wind direction change.

II. Methodology

A. Context and simulation

The Radioactive Dispersal Device (RDD), or dirty bomb [11],[12] simulation used Cs-137 as the source term, with an activity of 1.11E+17 Bq (3.0E+6 Ci) and a half-life of approximately 30 years, which is commonly employed in food sterilization [8]. Due to the short observation period (≈ 4 days) compared to the half-life of Cs-137, no correction was made for the radiation dose resulting from the radioactive decay of the source term. The estimated environmental radiation doses did not include the potential ballistic effects of the source term fragments, which were considered fully aerosolized in the explosion process.

The simulation was performed using general explosion (GE) mode, with 12 kg of TNT and conservative values of damage ratio (DR), airborne fraction (ARF), respirable fraction (FR), and leakage factor (LPF), considering that the radioactive material was wholly released. The sampling time was 10 minutes for receiver heights ≤ 1.5 m and all distances were conservatively estimated at the plume centerline, with 100% of the time considered to remain inside the plume—the mode of release, whether explosion or release in puffs, is not necessarily significant. The choice was made considering a mode with contamination capacity associated with other effects, such as the mechanical impact of the explosion, to make the scenario more challenging.

The isodoses were calculated to represent equal integral doses, and contamination plume areas were estimated by multiplying the mean population density by the plume areas, which play an essential role in estimating the size of the affected population. The plumes were categorized based on isodose values relevant to the study: (a) 700 mSv, which may be considered as the threshold for the occurrence of deterministic effects of radiation and the onset of acute radiation syndrome (ARS) [10]; (b) 100 mSv, as the limit for voluntarism in responding to the event and also the dividing line between high and low radiation doses [9]; and (c) 50 mSv, which is considered a limit for triggering local evacuation actions [9].

The study's scenario is typical of the initial phase of a response when accurate information is scarce (around the first 100 h). The primary threat is considered to be the simulated radiation field. However, it is essential to note that the HotSpot analytical model has certain limitations that must be considered. For instance, there is uncertainty associated with its spatial results. According to the developers, limiting the assessment to 10 km from the release point along the central axis of the ellipses representing the contamination plumes is recommended due to the limitations of the Pasquill-Gifford theory [7]. Additionally, other restrictions may arise from the typical built-up urban geometry, which analytical models may not address efficiently due to mathematical limitations when considering edge effects. Therefore, numerical methods may be a better option for more accurate results for smaller areas where greater detail is essential. It is worth mentioning that the simulation results are overestimated (conservative) and are helpful as a first-order approximation over the short period considered in the study. The fundamental mathematical principles of the Gaussian model, employed to compute concentrations in three-dimensional space and forecast the spread of a contamination plume, can also be found in HotSpot's manual [7].

B. Calculation of intersecting zones

A geometric approach to modeling the intersection zone is the Rose Curve, whose parametric equation in polar coordinates is given by Equation 1. This approach was chosen due to its similarity to the ellipses produced by HotSpot

$$r = L\cos(\omega) \qquad (1)$$

where L is the length of the central axis of the simulated ellipse, ω is a geometric factor related to the atmospheric stability class (PG), and θ is the parameter that maps the curve.

It is to be noted that even a minor variation in the wind speed or direction can result in an angular displacement in the plume. The current assumption in this work is that the wind speed remains nearly constant in intensity, and any changes are confined to its direction. Figure 1 introduces a schematic representation of the plume displacement.

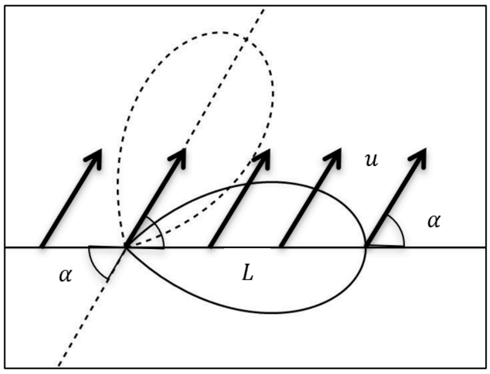

Fig. 1. Schematic representation of the plume displacement, L is the central axis of the simulated ellipse, and u and α are the wind speed and its direction about L.

Equation 2 models the new rotated position of the plume by changing the cosine argument by one phase, given the consideration in Figure 1

$$r' = L\cos(\omega(\theta+\alpha)) \qquad (2)$$

where α represents the rotation angle between the wind speed direction u, and the central axis L of the plume.

The equation for finding the intersection area of two identical Rose Curve petals (no changes in PG class), rotated by an angle, is given by Equation 3

$$A = \frac{L^2}{2}\int_{\theta_{min}}^{\theta_{max}} \cos^2(\omega(\theta + \alpha))d\theta + \frac{L^2}{2}\int_{\theta'_{min}}^{\theta'_{max}} \cos^2(\omega\theta)d\theta \qquad (3)$$

The two identical plumes in Equation 3 can be simplified using Equation 4

$$A = L^2 \int_{\theta'_{min}}^{\theta'_{max}} \cos^2(\omega\theta)d\theta \qquad (4)$$

where θ represents the wind direction, L is the central axis length of the ellipse, and ω is the geometric factor of the function [13].

The angles θ_{min} and θ_{max} determine the integration zone of a given area. This zone is where the integral will be applied. Most polar representations use sinusoids and cosines in their functions, which require a specified periodicity. The angles θ_{min} and θ_{max} are the points where two curves intersect, which makes for a better representation. The variable ω is often called the geometric factor. It simplifies the radiation dose calculation process, and our research group has recently achieved promising results using this approach [1]-[5]. Figure 2 provides a summary of the whole methodology.

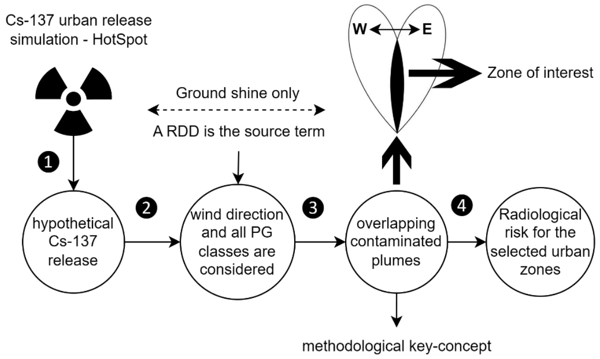

Fig. 2. Main methodological steps followed in the study.

III. Results and Discussion

The experiments involved changing the wind direction and the contamination plume by 30º toward the west (270º to 300º). By rotating the wind 30º to the west, we could define the integration limits in the polar coordinate plane (Equation 5). In this case, the limits (θ_{min} and θ_{max}) vary from 0 to (π/12). Table 1 contains the values of (ω) used for the approximation. Defining a specific integration region is necessary to accurately calculate the overlapping area between the rotated and non-rotated plume. The angles θ_{min} and θ_{max} mark the points where the two plumes intersect. These points represent precisely half of the intersection area. The value of θ_{max} should be varied from where the overlap between the plumes starts until it reaches the maximum height of the region to be computed. When calculating the overlapping area, the inversion between the intersection limit points was not considered, as it did not affect the physical result obtained. The geometric factor (ω) used for approximation can be found in Table 1.

TABLE I. Geometric factor (Ω) for each PG Class for all boundaries (outer, middle, and inner)

ω	*PG A*	*PG B*	*PG C*	*PG D*	*PG E*	*PG F*
outer	3	3	5	25	35	35
middle	5	5	8	30	40	40
inner	7	7	10	40	45	45

Using the overlap zone (transition), it is possible to identify where contamination plumes intersect based on the radiation dose values obtained in the simulation. This information is essential as it facilitates the effective management and mitigation of contamination, ensuring the preservation of public health and the environment. The rotating plumes' areas of intersection are subject to changes in atmospheric stability classes and wind direction, resulting in variable damage estimates. The size of the potentially affected population in the intersection region will fluctuate proportionally to the overlapping area's size. Figure 3 explores the impact of contamination plumes' rotation on public individuals and the effect of PG classes (A to F) on overlapping areas.

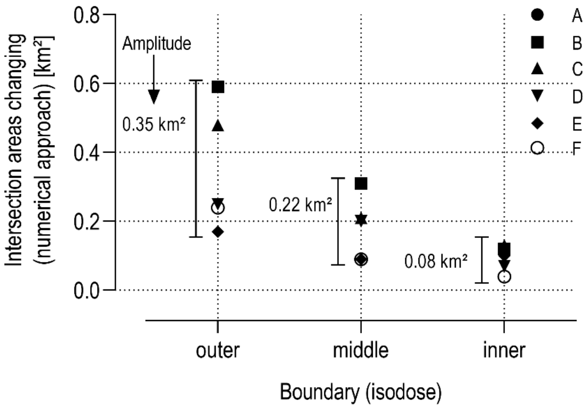

Fig. 3. The contamination plumes' intersection areas vary due to wind direction and PG classes.

The range of the differences between the areas of contaminated plumes that overlap can be calculated by subtracting the smallest size from the largest area within the boundaries of the plumes. These areas are determined based on the PG classes for each boundary - outer, middle, and inner - and then (conservatively) multiplied by the local demographic density. This calculation provides a conservative estimate that can be useful in the early stages of a crisis. For instance, if there are 10,000 inhabitants per square kilometer in an urban area affected by contamination, the excess number of inhabitants in the outer, middle, and inner boundaries would be approximately 3,500, 2,200, and 800, respectively.

Our group has conducted recent studies on building resilience in the face of disruptive events in the Chemical, Biological, Radiological, and Nuclear (CBRN) spectrum. We propose using modeling techniques to assess the impact of such events on the maintenance of urban functioning [2]-[3]. Our prospective studies aim to compare numerical and analytical computational simulations to generate dimensionless factors that can balance the prediction equations. This balance can be essential for developing coping strategies, prioritizing goals, and supporting decision-making.

The study is focused on developing a methodology for conservatively assessing environmental radiological contamination. This methodology is being adapted to complement the ARGOS code [6], enabling us to compare analytical and numerical assessments for a contamination event. The findings can be applied realistically to support decision-making in CBRN environmental contamination cases in urban and rural contexts. The approach may help decision-makers respond to a disruptive event more effectively, aiming to reduce harm to the population and the environment.

IV. Conclusion

The overlapping areas result from changes in Pasquill-Gifford classes and wind direction. These overlapping zones require heightened attention during field activities and prioritization processes, as they indicate higher contamination levels and pose increased risks to the population and the environment. The appearance of these zones of heightened exposure (overlapping) and their dynamics varies based on the intensity of variations in PG classes. It is conceivable that the methodology and its findings could be better suited for predictive assessments rather than real-time ones. However, the methodology could also be utilized in real-time scenarios.

REFERENCES

[1] Andrade, E.R., Alves, I.S., Carolina Lodi Lobato, A., Stenders, R.M., Curzio, R.C., Bonfim, C.E.S., 2021. Life-shortening effects of radiological weapons in military operations. The Journal of Defense Modeling and Simulation 0, 15485129211064265.

[2] Andrade, E.R., Reis, A.L.Q., Alves, D.F., Alves, I.S., Andrade, E.V.S.L., Stenders, R.M., Federico, C.A., Silva, A.X., 2020. Urban critical infrastructure disruption after a radiological dispersive device event. Journal of Environmental Radioactivity 222, 106358.

[3] Andrade, E.R., Reis, A.L.Q., Stenders, R.M., Vital, H.C., Rebello, W.F., Silva, A.X., 2022. Evaluating urban resilience in a disruptive radioactive event. Progress in Nuclear Energy 147, 104218.

[4] Brum, T., Lima, S.X., Amorim, J.C.C., Stenders, R.M., Prah, M., Vital, H.C., Andrade, E.R., 2020. Immediate decisions are based on long-term consequence evaluation for a radiological event. The Journal of Defense Modeling and Simulation 18, 365-373.

[5] Curzio, R.C., Bonfim, C.E.S., Silva, T.M.S., Stenders, R.M., Ramos de Andrade, E., 2023. Dose assessment based on short-ranged computer simulation in a radioactive release event. Radioprotection 58, 197-204.

[6] Hoe, S., McGinnity, P., Charnock, T., Gering, F., Schou Jacobsen, L.H., Havskov Sorensen, J., Andersson, K., Astrup, P., 2010. ARGOS decision support system for emergency management. IAEA, International Atomic Energy Agency (IAEA).

[7] Homann, S.G., Aluzzi, F., 2020. HotSpot Health Physics Codes Version 3.1.2 User's Guide. Lawrence Livermore National Laboratory, CA, USA.

[8] IAEA, 2005. Categorization of Radioactive Sources, IAEA SAFETY STANDARDS SERIES No. RS-G-1.9. INTERNATIONAL ATOMIC ENERGY AGENCY, Vienna.

[9] ICRP, 2007. The 2007 Recommendations of the International Commission on Radiological Protection. ICRP publication 103. Annals of the ICRP 37, 1-332.

[10] Isabela S. Alves, Mariana S.C. Castro, Ricardo M. Stenders, Rodrigo W. Silva, Tercio Brum, Ademir X. Silva, Edson R. Andrade, 2019. The vertical radiation dose profile and decision-making in a simulated urban event. Journal of Environmental Radioactivity 208-209, 106034.

[11] Karam, P., 2005. Radiological Terrorism. Human and Ecological Risk Assessment - HUM ECOL RISK ASSESSMENT 11.

[12] Karam, P.A., 2021. Radiological and Nuclear Terrorism: Their Science, Effects, Prevention, and Recovery. Springer International Publishing.

[13] LeVeque, R.J., 2005. Finite Difference Methods for Differential Equations. University of Washington.